Estimation of OH in urban plume using TROPOMI inferred NO_2/CO

Srijana Lama[1], Sander Houweling[1,2], K. Folkert Boersma[3,4], Ilse Aben[2,1], Hugo A. C. Denier van der Gon[6], Maarten C. Krol[3,7]

[1]Vrije Universiteit, Department of Earth Sciences, Amsterdam, the Netherlands
[2]SRON Netherlands Institute for Space Research, Leiden, the Netherlands
[3]Wageningen University, Meteorology and Air Quality Group, Wageningen, the Netherlands
[4]Royal Netherlands Meteorological Institute, R&D Satellite Observations, de Bilt, the Netherlands
[6]TNO, Department of Climate, Air and Sustainability, Princetonlaan, the Netherlands
[7]Institute for Marine and Atmospheric Research Utrecht, Utrecht University, Utrecht, the Netherlands

Corresponding author: Srijana Lama (s.lama@vu.nl, sreejanalama@gmail.com)

Contents of this file

Text S1 to S5
Figures S1 to S20
Tables S1 to S4

Text S1. Least square optimization

We have model M to simulate data d_{mod} with the given model parameter x

$d_{mod} = M(x)$

For the non-linear case, the model search the most probable solution of x at the minimum of cost function (J) .

$$J_{(x)} = \frac{1}{2}.\left[\left(d_{obs} - M(x)\right)^{T} R^{-1}\left(d_{obs} - M(x)\right) + (x - x_0)^{T} B^{-1}(x - x_0)\right]$$

$$R = \begin{bmatrix} \sigma_{d1}^2 & . & cov(d3,d1) \\ . & \sigma_{d2}^2 & . \\ cov(d1,d3) & . & \sigma_{d3}^2 \end{bmatrix} \quad B = \begin{bmatrix} \sigma_{dx1}^2 & . & cov(x3,x1) \\ . & \sigma_{dx2}^2 & . \\ cov(x1,x3) & . & \sigma_{x3}^2 \end{bmatrix}$$

The cost function has two terms, the first measures the distance between the observations(d_{obs}) and the model (M), the second measures the distance between the parameter(x) solution and its first guess (x_0). R and B are the covariance matrices for d_{obs} and x, showing their uncertanity.

Text S2. Derivation of EMG method

$\tau_{NO2} = \frac{x_o}{U}$

xo is the downwind decay length [km] obtained from EMG method and U [m/s] is the boundary layer averaged wind speed for the box 100kmx400km. The unit of lifetime is hr .

$\tau_{NO2} = \frac{1}{K_{NO2\,OH}[OH]}$

Converting the hour into second

τ_{NO2}*60.0*60.0 $= \frac{1}{K_{NO2\,OH}[OH]}$

OH $= \frac{1}{\tau_{NO2}*60.0*60.0*\,K_{NO2\,OH}}$

$K_{NO2\,OH}$ is the IUPAC second order rate constant [s^{-1}molecules^{-1}cm^3] and OH [moleculescm^{-3}] is the hydroxyl radical concentration over Riyadh at time TROPOMI overpasses.

Text S3. Conversion of NO_2 emission in molecule cm^{-1} into mole second^{-1}

$E_{NO2} * U$

Converting the ms^{-1} into cm s^{-1} and molecules into moles

$\frac{E_{NO2}*U*100}{6.023e^{23}}$

E_NO_2 is the NO_2 emission [molecule cm^{-1}] obtained from EMG method. U[m s^{-1}] is the wind speed.

Text S4. X^2 calculation

$$X^2 = \sum_{i=1}^{n} \frac{(\text{Observed}_i - \text{expected}_i)^2}{\text{expected}_i}$$

Observed data is TROPOMI output and expected data is the results of WRF optimization

Text S5. Uncertainty estimation on OH concentration, NO_x and CO emission using least square method and EMG method

For the error calculation, the relative change in the OH concentration, NO_x and CO emission with alteration in the width of box, downwind length of box , wind speed and NO_2 bias correction is estimated. The width of the box is changed from 100km to 90 km and 110km. Downwind length of box is changed from 200km to 190km and 210km. For the effect of wind speed, we used WRF wind data and compare the results with the CAMS wind data. To estimate the error from NO_2 bias correction, we increase and decrease bias corrected NO_2 by 5 % in the city plume. The total uncertainties is derived by adding the contribution of individual component in quadrature.

Table S1. Estimated uncertainties in f_{emis} , f_{OH} and f_{Bg} obtained by ratio optimization of XNO_2 and XCO for summer and Winter over Riyadh.

	Uncertainty Summer (%)			Uncertainty Winter (%)		
	OH	Emission ratio	Bg ratio	OH	Emission ratio	Bg ratio
Width of the box (A)	4.8	2.5	1.0	8.2	16.0	4.1
Downwind length (B)	4.5	3.2	1.7	4.0	12.0	3.0
Wind speed (C)	8.4	8.4	8.4	4.1	4.1	4.1
NO2 Bias Correction (D)	2.4	0.50	1.2	4.9	53.0	1.0
Total Uncertainty $(\sqrt{(A^2 + B^2 + C^2 + D^2)}$ **(%)**	11.0	9.3	8.7	11.1	56.8	6.6

Table S2. Same as Table S1 but the estimated uncertainties in f_{emis} , f_{OH} and f_{Bg} obtained by component wise optimization of XNO_2 and XCO.

	Uncertainty Summer (%)					Uncertainty Winter (%)				
	OH	NO_x Emission	NO_x Bg	CO Emission	CO Bg	OH	NO_x Emission	NO_x Bg	CO emission	CO Bg
Width of the box (A)	5.8	10.0	9.8	9.1	8.7	8.1	6.5	4.1	9.4	4.5
Downwind length (B)	4.5	4.5	1.5	0.9	0.2	2.9	3.4	3	1.4	0.5
Wind speed (C)	8.4	8.4	8.4	8.4	8.4	4.1	4.1	4.1	4.1	4.1
NO_2 Bias Correction (D)	2.4	17.9	1.0	x	x	3.0	20.4	1.0	X	x

Total Uncertainty $(\sqrt{(\mathbf{A^2 + B^2 + C^2 +}}$ **(%)**	11.4	22.6	13.0	12.4	11.6	10.0	22.1	6.7	10.4	6.1

Table S3. Same as Table S1 but the estimated uncertainties in OH and NO_x emission obtained by EMG method

	Uncertainty Summer (%)		Uncertainty Winter (%)	
	OH	Emission	OH	Emission
Width of the box (A)	4.0	7.5	4.0	10.0
Downwind length (B)	2.0	2.5	2.0	10.0
Wind speed (C)	8.4	8.4	4.1	4.1
NO2 Bias Correction (D)	5.0	7.0	4.4	25.0
Total Uncertainty (%) $(\sqrt{(\mathbf{A^2 + B^2 + C^2 + D^2})}$	10.8	13.5	7.5	29.0

Table S4. Comparison of EDGAR CO emission 2012, 2018 with the Optimized CO emission over Riyadh at the time TROPOMI overpasses. Emission presented below includes diurnal, weekly and monthly emission factor.

	2012		2018		OPTIMIZED EMISSION	
	Summer	Winter	Summer	Winter	Summer	Winter
CO emission (kg/s)	11.9	11.7	16.4	14.4	23.8	23.4

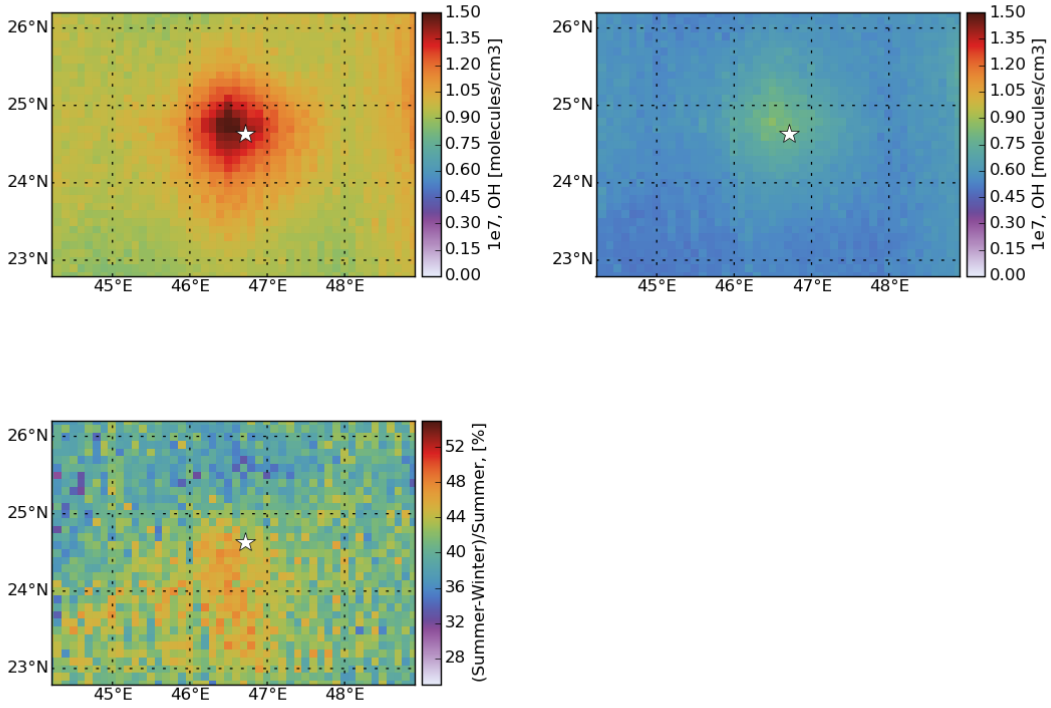

Figure S1. Boundary layer averaged CAMS OH concentration a) Summer, b) Winter and c) Relative difference over Riyadh at the time TROPOMI overpasses.

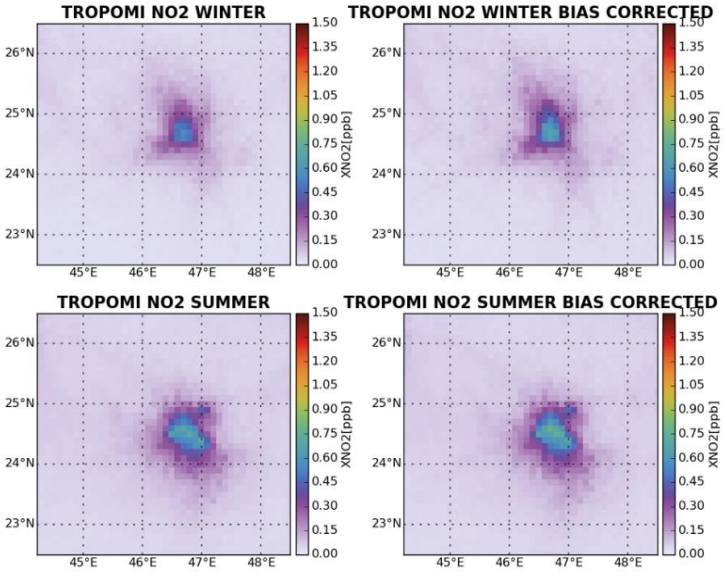

Figure S2. TROPOMI derived XNO2 before and after bias correction using AMF recalculation for summer (bottom) and winter (top) over Riyadh.

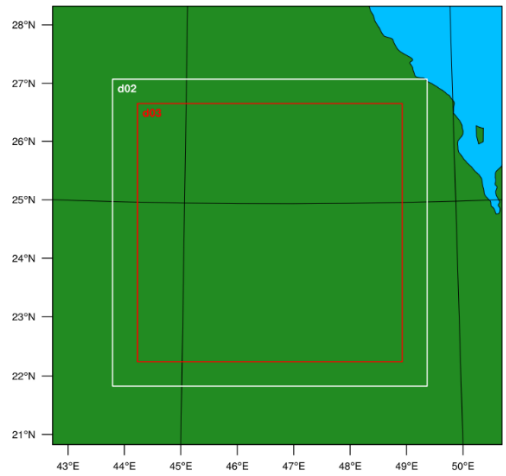

Figure S3. WRF domains d01, d02 and d03 with the spatial resolutions of 27km, 9km and 3 km over Riyadh

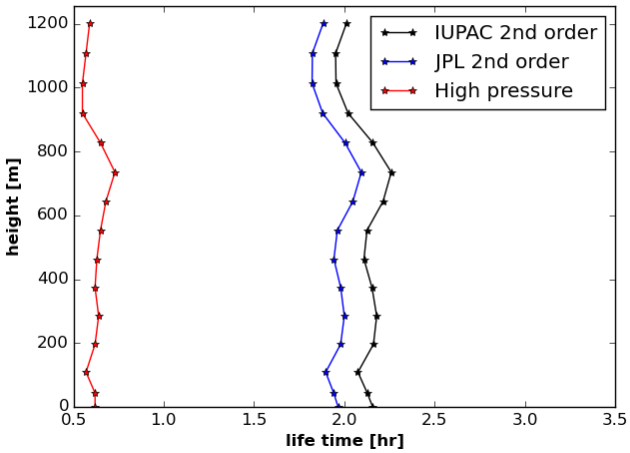

Figure S4. Lifetime profile for high pressure rate constant, JPL 2nd order and IUPAC 2nd order rate constant at the center of Riyadh

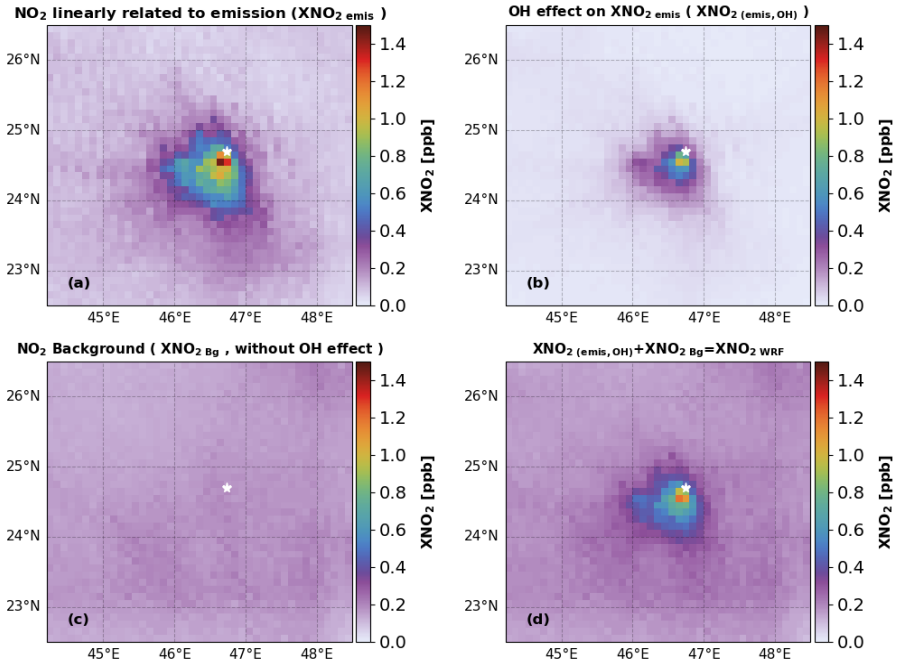

Figure S5. WRF simulated NO_2 a) linearly related to emission $\left(XNO_{2,emis}\right)$ b) OH effect on $XNO_{2,emis}$ ($XNO_{2,(emis,OH)}$) c) NO_2 background based on CAMS $\left(XNO_{2\,Bg}\right)$ and d) sum of $XNO_{2,(emis,OH)}$ and $XNO_{2\,Bg}$ to derive $XNO_{2\,WRF}$ over Riyadh averaged from June to October, 2018.

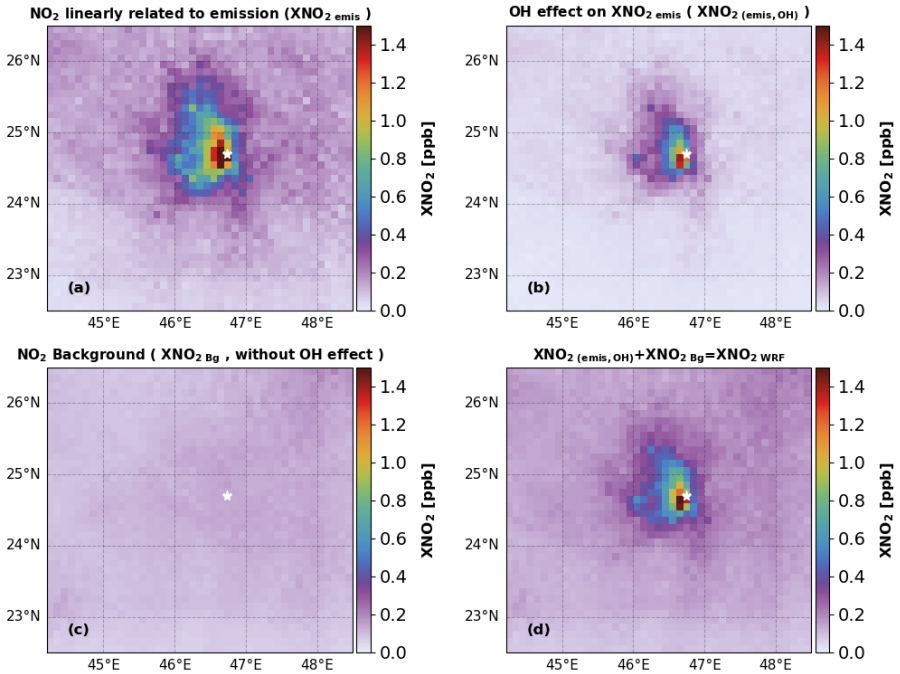

Figure S6. Same as Fig. S5 but for winter (November, 2018 to March, 2019)

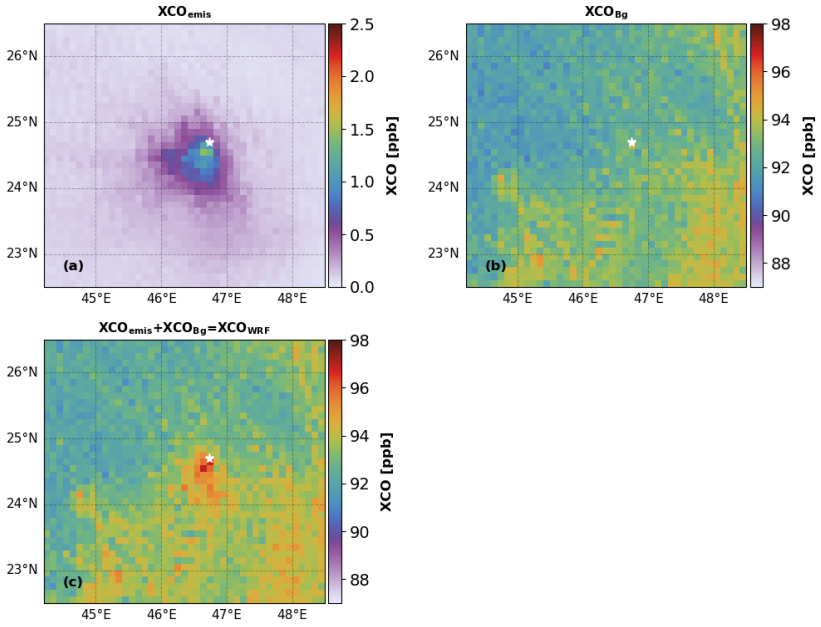

Figure S7. WRF simulated CO a) linearly related to emission (XCO_{emis}), b) background based on CAMS (XCO_{Bg}) and c) sum of XCO_{emis} and XCO_{Bg} to derive XCO_{WRF} over Riyadh averaged from June to October, 2018.

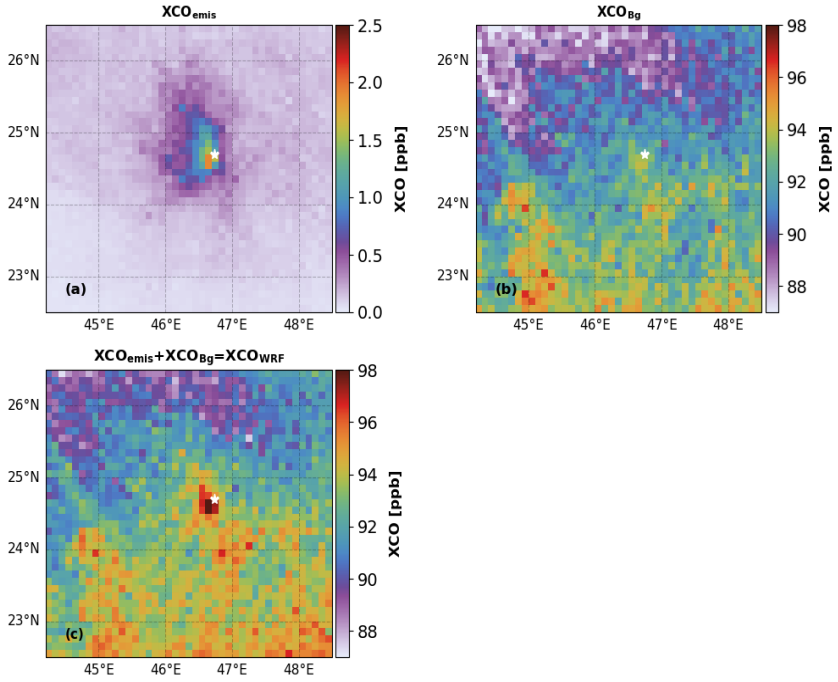

Figure S8. Same as Fig. S7 but for winter (November, 2018 to March, 2019)

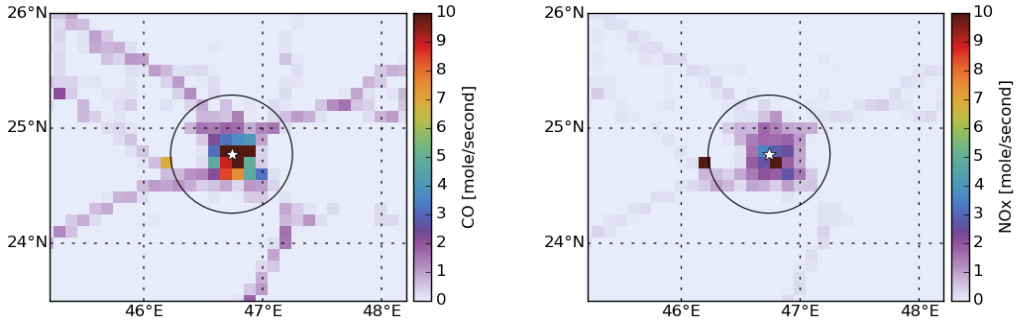

Figure S9. EDGAR 2012 CO (left) and NOx (right) emission over Riyadh. The white star represents the center of Riyadh.

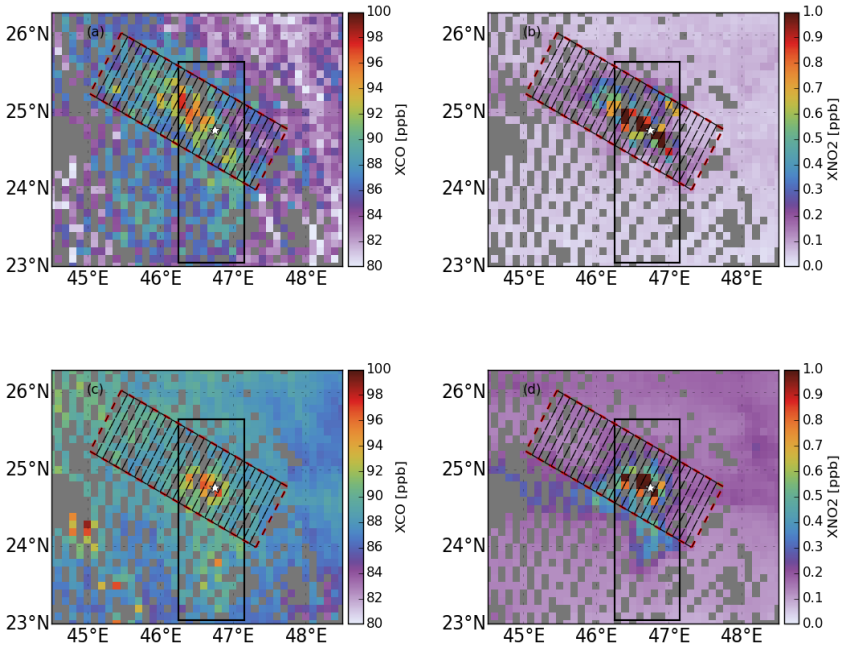

Figure S10. TROPOMI derived a) XCO, b) XNO2 and WRF derived c) XCO and d) XNO2 over Riyadh for 4th August, 2018. The white star represents the centre of Riyadh. The black box (B1) with a dimension of 300kmx100km is rotated depending upon the average wind direction 50 km radius from the centre of Riyadh at the TROPOMI overpasses resulting red box. For the calculation of zonally averaged NO2 and CO, red box is divided into 29 smaller cells with the width (dx) ~11km. TROPOMI and WRF derived XCO and XNO2 is gridded at 0.1°x0.1°.

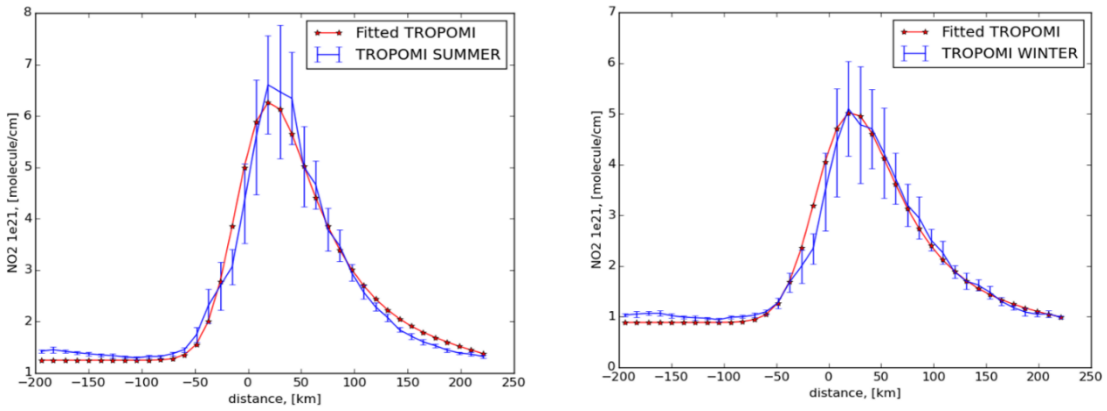

Figure S11. Zonally averaged NO2 tropospheric column densities (mean ±SME) for North east wind as a function of the distance over Riyadh (420 kmx250 km) for summer (left) and winter (right). The red line represents the fitted NO_2 column densities using EMG method. The correlation between observation and fit for summer is r^2= 0.94 and for winter is r^2= 0.96.

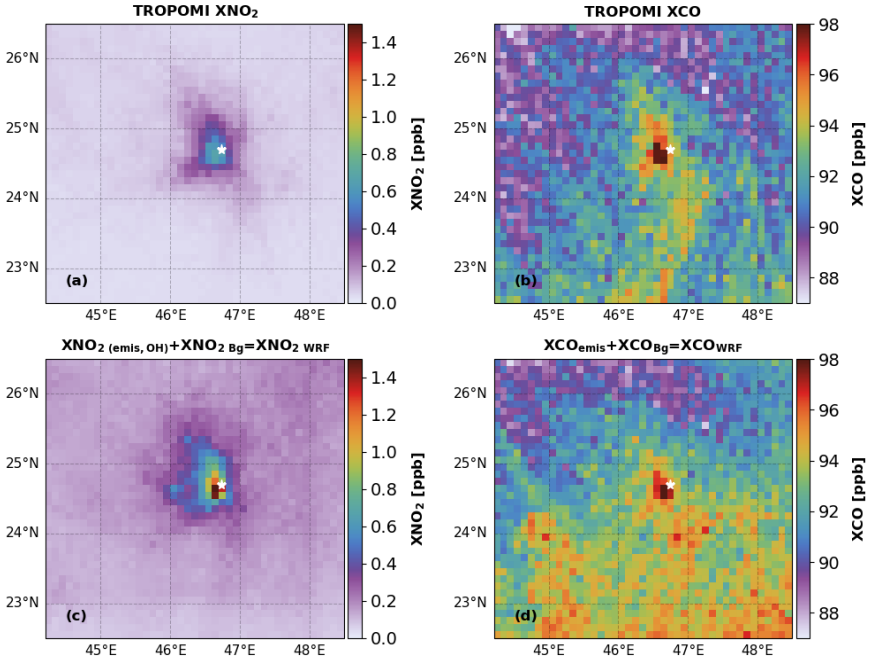

Figure S12. Co-located TROPOMI derived a) XNO2 and b) XCO for November, 2018 to March, 2019 over Riyadh. Temporally, bilinear and vertically interpolated WRF simulated c)$XNO_{2\ WRF}$ and d) $XCO_{\ WRF}$ at the resolution of TROPOMI. The white star represents the centre of city. TROPOMI and WRF results are gridded at 0.1˚x0.1˚

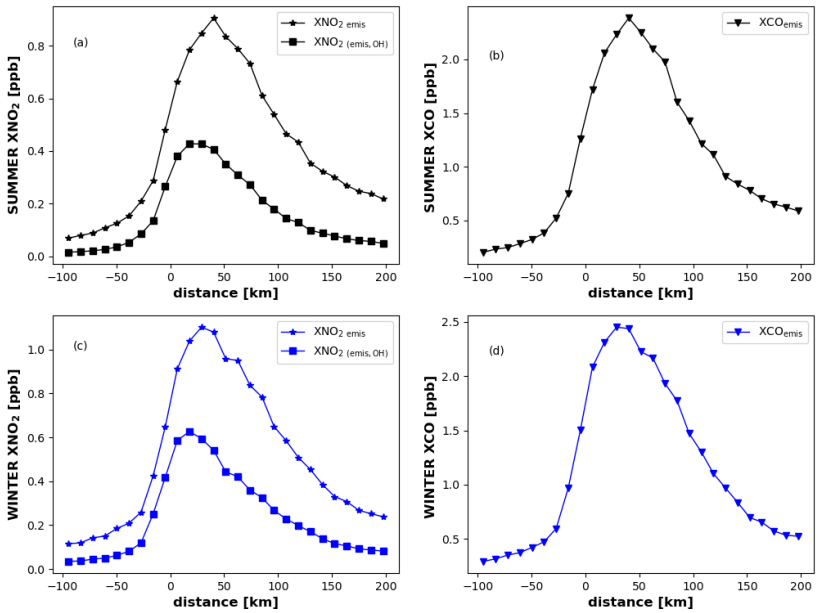

Figure S13. Zonally averaged a) summer $XNO_{2\ emis}$ and $XNO_{2\ (emis\ ,\ OH)}$, b) summer XCO_{emis}, c) winter $XNO_{2\ emis}$ and $XNO_{2\ (emis\ ,\ OH)}$ and d) winter XCO_{emis}. For the function of each of the tracer see Table 1.

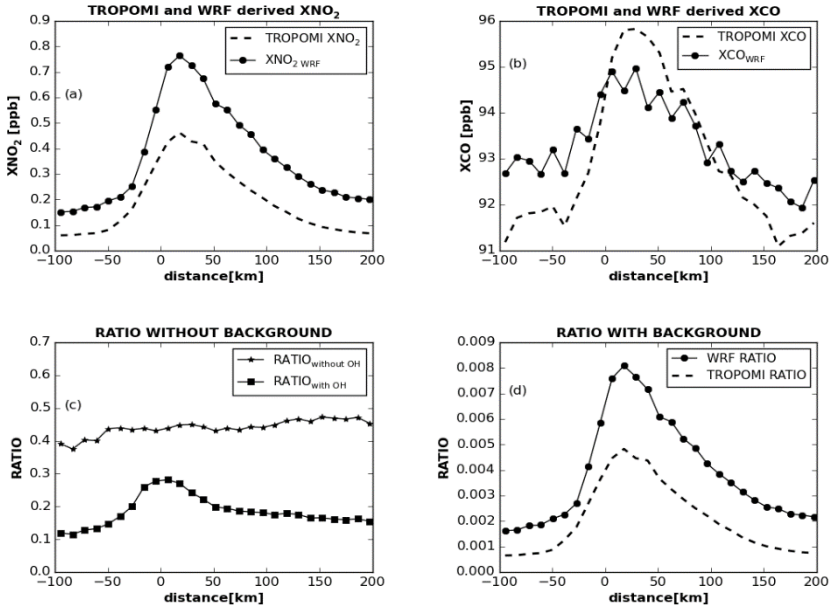

Figure S14. Comparison of WRF and TROPOMI zonally averaged a) XNO2, b) XCO and c) WRF Ratio (XNO_2/ XCO) without CAMS background d) TROPOMI and WRF Ratio (XNO_2/ XCO) with background as a function of distance to the centre of Riyadh for winter (November, 2018 to March, 2019).

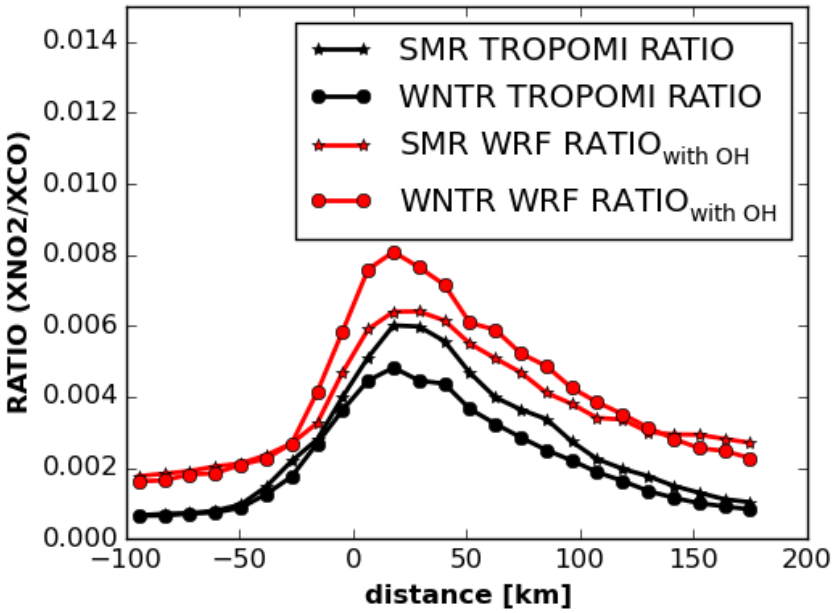

Figure S15. Comparison of WRF and TROPOMI derived Ratio (XNO_2/ XCO) as a function of distance to the centre of Riyadh for summer and winter.

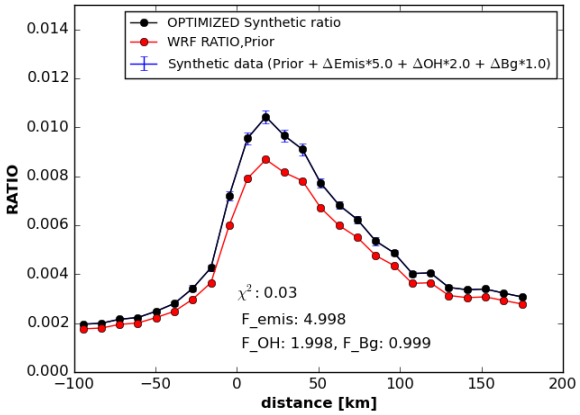

Figure S16. Summer (June to October,2018) averaged WRF derived Ratio before and after optimization in comparison to synthetic data (data ±std). F_{emis}, F_{OH} and F_{Bg} represents the factor for emission, OH and background by which synthetic data is higher compared to WRF ratio.

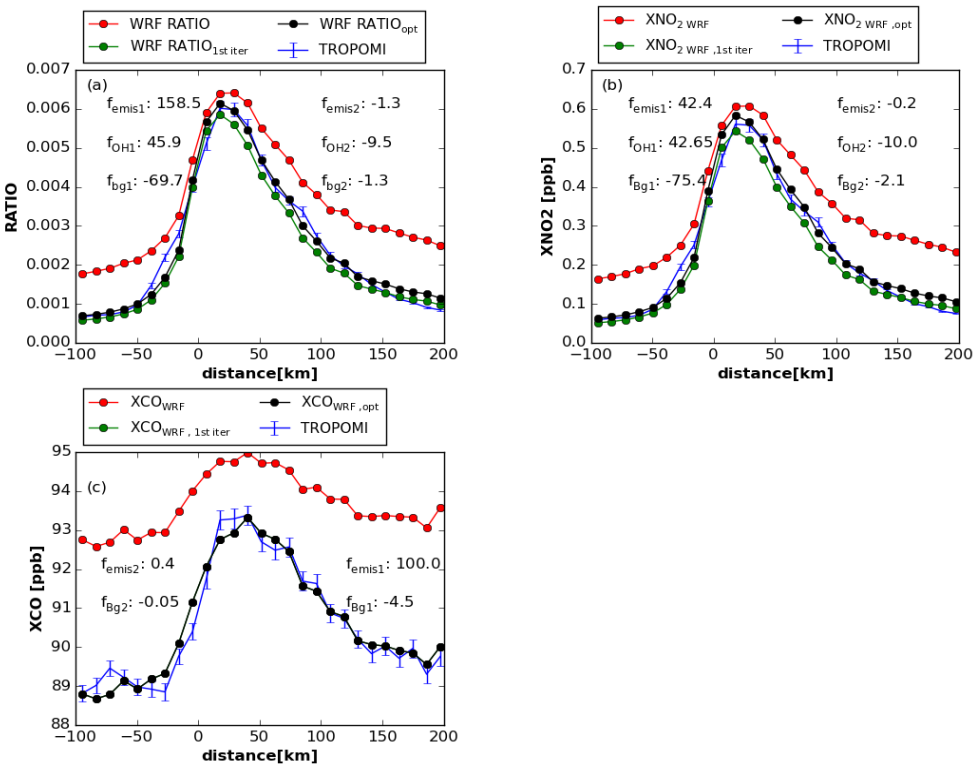

Figure S17. Summer (June, 2018 to October ,2018) averaged WRF derived a) Ratio, b) XNO2 and c) XCO in comparison to TROPOMI. Step1: f_{OH1}, f_{emis1} and f_{Bg1} is the first scaling factor for OH, emission and background derived from least square method while comparing WRF prior run to TROPOMI. Step2: Change the emission , background and OH used in prior run by applying f_{OH1}, f_{emis1} and f_{Bg1} and derive WRF Ratio $_{1st\ iter}$, $XNO_{2\ 1st\ iter}$ and $XCO_{WRF,\ 1st\ iter}$. Step 3: f_{OH2}, f_{emis2} and f_{Bg2} second scaling factor derived from least square method while comparing the result of 1st iteration to TROPOMI. Step 4: Apply f_{OH2}, f_{emis2} and f_{Bg2} to the emission, background and OH concentration used for 1st iteration and derive WRF $Ratio_{opt}$, $XNO_{2\ WRF,opt}$. To get the final scaling factor, divide the results of 2nd iteration by Prior run.

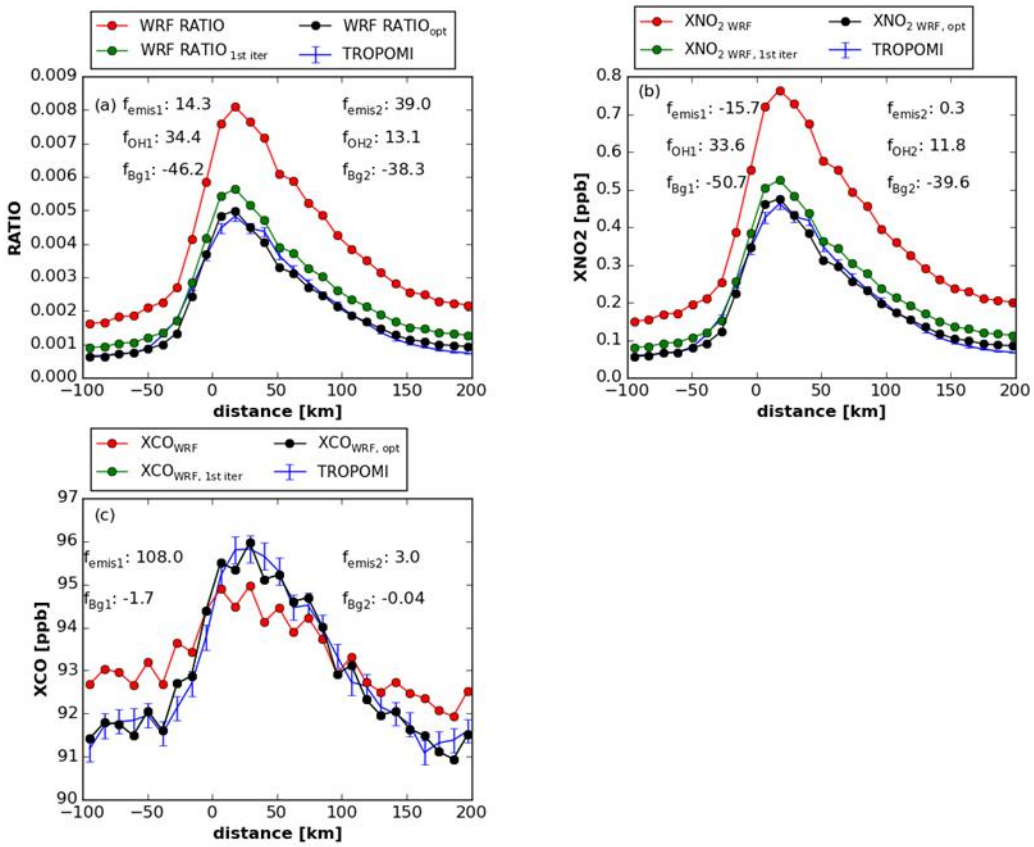

Figure S18. Same as Figure S10 but for Winter (November, 2018 to March,2019).

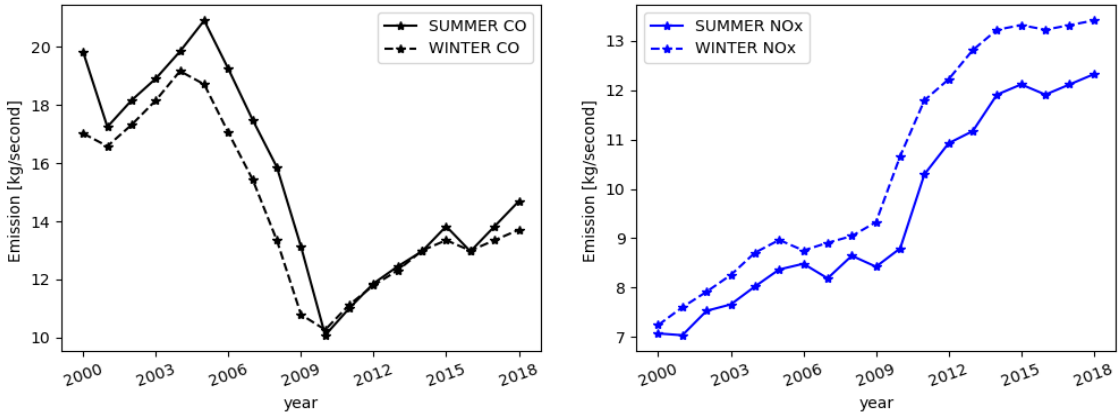

Figure S19. EDGAR a) CO and b) NOx emission from 2000 to 2018 for summer and winter at the time TROPOMI overpasses over Riyadh. EDGAR 2000 to 2015 data is linearly extrapolated to derived emission data for 2018.

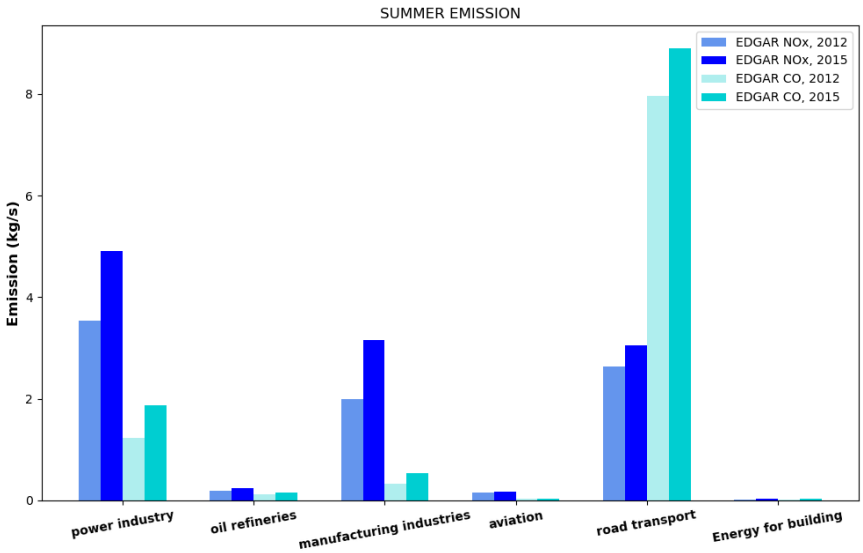

Figure S20. EDGAR NOx and CO emission for different source sectors for summer 2012 and 2015 at the time TROPOMI overpasses over Riyadh.